A new method for the adaptive control of vortex-wall interactions

By P. Koumoutsakos

1. Motivation and objectives

The control of vortical flows is gaining significance in the design of aeronautical and marine structures. While passive devices have been used effectively in the past, active control strategies have the potential of allowing a leap in the performance of future configurations. The efficiency of control schemes is strongly dependent on the development of accurate flow models that can be devised using information that is available not only from numerical solutions of the governing Navier-Stokes equations but also can be measured experimentally. In that context it is desirable to construct adaptive control schemes using information that can be measured at the wall.

The objective of this study is to propose an efficient methodology for the adaptive control of vortical, wall bounded flows. The present scheme is based on sensing wall pressure and calculating the wall vorticity flux from this information. This information is used to determine the amount of unsteady, spatially varying mass transpiration needed as the actuating mechanism. The amount of suction and blowing is determined explicitly in order to achieve a desired vorticity flux at the wall. The closed form control law is obtained by formulating the physical mechanism of vorticity generation at a no-slip wall.

The control scheme is tested on the model problem of a vortex dipole impinging on a wall. It is shown that by using information at the wall, we are able to reproduce efficiently the effects obtained by other control schemes that rely on off-wall information. The proposed methodology is based on explicit formulation of physical processes, and its simplicity allows its incorporation to flow control both computationally as well as in actual applications.

The control scheme is discussed in more detail in Koumoutsakos (1996); only representative results are presented in this report.

2. Accomplishments

2.1 Wall-vorticity flux

In wall bounded flows, the tangential velocity of fluid elements relative to the boundary establishes velocity gradients. With the definition of vorticity ($\boldsymbol{\omega}$) as the curl of velocity ($\boldsymbol{\omega} = \nabla \times \mathbf{u}$), this may be equivalently described in terms of the vorticity that is acquired by the fluid elements near the wall. Lighthill (1963) envisioned the wall as a system of sources and sinks of vorticity. He drew an analogy between the way vorticity is produced at the wall and enters the flow and the way temperatures are established near a heat conducting boundary.

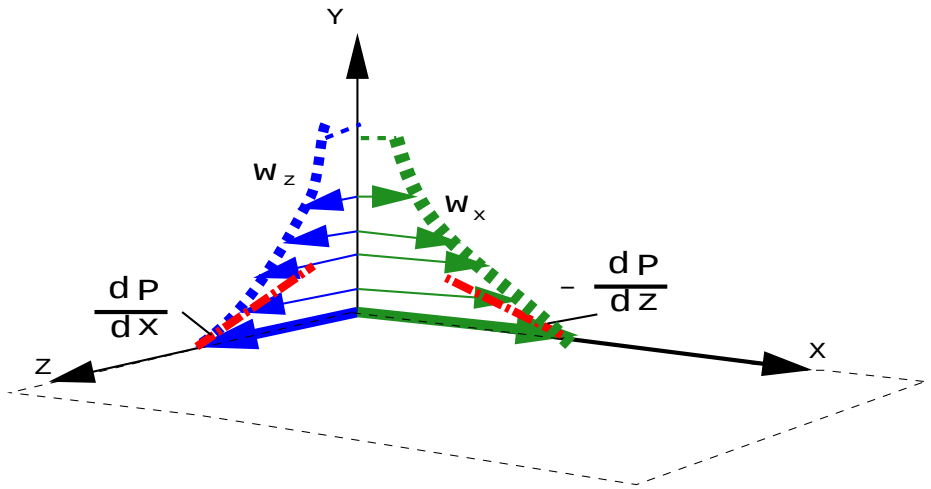

FIGURE 1. Definition sketch.

Following Hornung (1990) we identify the *diffusive vorticity flux tensor at the wall* as:

$$J_w \;=\; -(\nu\nabla\boldsymbol{\omega})_{\mathrm{w}} \tag{1}$$

where ν is the kinematic viscosity of the fluid and the subscript w denotes quantities measured at the wall.

The normal component of the diffusive vorticity flux tensor is defined as the wall vorticity flux (Panton 1984, Hornung 1990).

$$\boldsymbol{\sigma} \;=\; -\,(\nu\mathbf{n}\cdot\nabla\vec{\boldsymbol{\omega}})_{\mathrm{w}} \tag{2}$$

where $\boldsymbol{\omega}$ is the vorticity and $\mathbf{n}$ is the outward normal at the wall.

In the rest of this work we consider for simplicity a Cartesian coordinate system and flow over a flat wall identified with the xOz plane (Fig. 1) with a unit normal $\widehat{j}$. The vorticity flux is then expressed as

$$\boldsymbol{\sigma} \;=\; -\left(\nu\frac{\partial\boldsymbol{\omega}}{\partial \mathrm{y}}\right)_{\mathrm{w}} \tag{3}$$

Hornung (1990) has presented a formula for the local vorticity flux for a general fluid material:

$$\boldsymbol{\sigma} \;=\; -\widehat{j}\times\left(\frac{\mathrm{d}\vec{\mathrm{V}}_{\mathrm{w}}}{\mathrm{dt}} \;+\; \frac{(\nabla \mathrm{p})_{\mathrm{w}}}{\rho_{\mathrm{w}}}\right) \;-\; \frac{1}{\rho_{\mathrm{w}}}\,\widehat{\mathrm{j}}\,\left(\widehat{\mathrm{j}}\cdot(\nabla\times\tau_{\mathrm{w}})\right) \;+\frac{1}{\rho_{\mathrm{w}}}\,\widehat{\mathrm{j}}\times\begin{bmatrix}\frac{\partial\sigma_{\mathrm{x}}}{\partial \mathrm{x}}\\ \frac{\partial\sigma_{\mathrm{z}}}{\partial \mathrm{z}}\\ 0\end{bmatrix} \tag{4}$$

where $\vec{V}_w(t)$ is the local wall velocity, τ_{w} is the shear stress tensor, and $\sigma_{\mathrm{x}}, \sigma_{\mathrm{z}}$ are the components of the normal stress components along the wall.

For an incompressible viscous flow over a stationary wall, the vorticity flux is directly proportional to the pressure gradients, as Eq. 4 reduces to:

$$\nu\left(\frac{\partial\omega_{\mathrm{x}}}{\partial \mathrm{y}}\right)_{\mathrm{w}} \;=\; \frac{1}{\rho}\left(\frac{\partial \mathrm{p}}{\partial \mathrm{z}}\right)_{\mathrm{w}} \quad\text{and}\quad -\,\nu\left(\frac{\partial\omega_{\mathrm{z}}}{\partial \mathrm{y}}\right)_{\mathrm{w}} \;=\; \frac{1}{\rho}\left(\frac{\partial \mathrm{p}}{\partial \mathrm{x}}\right)_{\mathrm{w}} \tag{5}$$

where p is the pressure and ω_x and ω_z are the streamwise and spanwise vorticity components (Fig. 1). The flux of the wall normal vorticity, ω_y, may be determined from the kinematic condition ($\nabla \cdot \boldsymbol{\omega} = 0$) as:

$$-\left(\frac{\partial \omega_y}{\partial y}\right)_w = \left(\frac{\partial \omega_x}{\partial x}\right)_w + \left(\frac{\partial \omega_z}{\partial z}\right)_w \tag{6}$$

Thus one may obtain the wall flux of all three vorticity components as a function of time by measuring the instantaneous pressure at the wall and calculating its gradient.

Wall pressure fluctuations measurements are often reported in the literature (see for example Johanson *et al.* 1987) and have revealed a strong coupling between the vortical structures near the wall and the pressure field on the wall. Similar observations have been made in flow fields obtained in direct numerical simulations of wall bounded flows (Moin and Kim, 1985). However, measurements of pressure gradients at a wall are not common. An exception is the work of Andreopoulos and Agui (1996) (referred to as AA from here on). They use high frequency response transducers to measure fluctuating wall pressure gradients and then compute the vorticity flux in a two-dimensional turbulent boundary layer. Their measurements demonstrated the significance of vorticity flux in describing near wall processes. They made an attempt to correlate vorticity flux signals with physical phenomena such as bursting-sweep processes in the boundary layer. They observed that fluid acquires or loses vorticity at the wall during rather violent events followed by periods of small fluctuations. During these events they observed a predominant orientation at 45^0 for the wall vorticity flux, implying an equal vorticity flux for the streamwise and the spanwise vorticity components. This may be linked with the observations of Orlandi and Jiménez (1994), who studied the role of spanwise vorticity in the redistribution of streamwise vortices and the formation of streaks of high and low skin friction in the boundary layer.

AA demonstrated that the major contributions to the vorticity flux come from the uncorrelated part of the pressure signals at two adjacent locations which contain a wide range of vortical scales. As the degree of correlation is smaller between the small scales, their contribution to the vorticity flux is more pronounced. This imposes a severe requirement on the spatial resolution of the pressure gradients/vorticity flux measurements. Practical applications would require actuators and sensors with sizes in the order of $50\mu m$ and actuator frequencies of 1MHz (Moin and Bewley, 1994). However, recent advances in micro pressure sensor fabrication technology (Ho and Yui 1996) give us an opportunity to overcome these difficulties. Löfdahl *et al.*, (1996) presented measurements in a two-dimensional flat plate boundary layer with a resolution of eddies with wave numbers less than ten viscous units using microscopic silicon pressure transducers. It appears that by using this new technology one may be able to describe in detail physical processes in terms of the flow vorticity and the wall vorticity flux.

The role of the vorticity flux from oscillating walls as a mechanism for the control of unsteady separated flows was discussed by Wu, Wu and Wu (1993). They

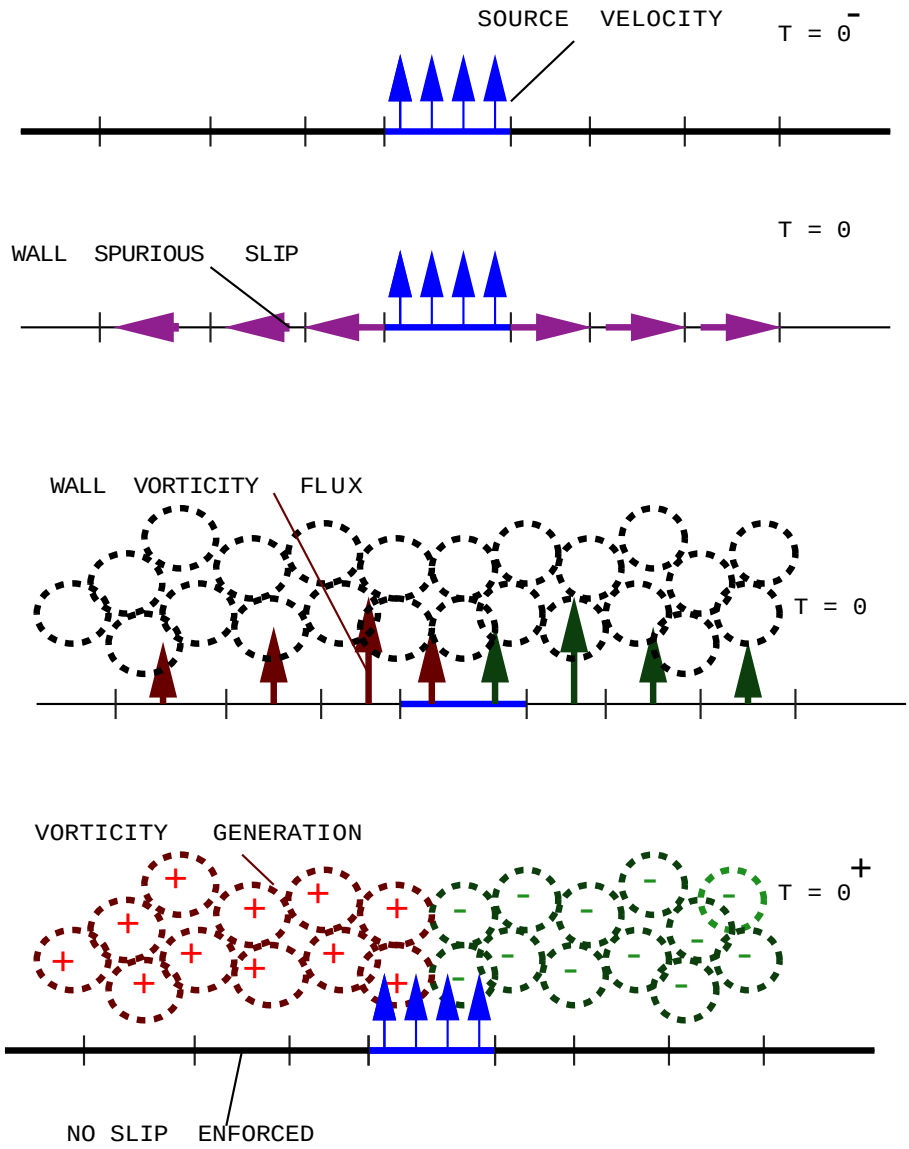

FIGURE 2. Slip cancellation algorithm.

concluded that wall oscillations can produce a mean vorticity flux that is partially responsible for phenomena of vortex flow control by waves. Gad-El-Hak has shown that the vorticity flux can be affected by wall transpiration as well as by wall-normal variation of the kinematic viscosity (ν) as a result of surface heating, film boiling, cavitation, sublimation, chemical reaction, wall injection of higher/lower viscosity fluid, or in the presence of shear thinning/thickening additive.

However these works do not provide us with an explicit formulation for the actuator strength necessary to induce a desired vorticity flux at the wall. In that direction, recently Lee, Kim, Babcock and Goodman (1996) used non-linear neural networks to obtain a simple expression for the wall blowing and suction needed to reduce the skin friction of turbulent channel flow.

In this article we propose the use of vorticity flux for effective, adaptive control

mechanisms in wall bounded flows. For a general fluid material the wall vorticity flux may be affected by appropriately selecting the type, magnitude, and location of the controlling devices so as to modify the fluid stresses near the wall (Eq. 9). For the present scheme using a formulation based on Lighthill's (1963) conceptual model of vorticity generation at the wall, we obtain in closed form the magnitude of the blowing/suction necessary to manipulate the vorticity field. The present control scheme relies on information that can be obtained experimentally as well as computationally. It is applied to the model problem (Choi, Moin and Kim, 1994 and referred to as CMK from here on) of a vortex dipole interacting with a wall. It is shown that the present strategy, using wall only information, reproduces efficiently phenomena that have been obtained previously using off wall information.

2.2 Vorticity flux induced by blowing and suction at the wall

We proceed to describe our methodology by considering two-dimensional configurations. The present analysis and the results discussed herein are readily extendable to three-dimensional flows.

Following Lighthill (1963) we consider the generation of vorticity at the wall as a fractional step algorithm. During the first substep an inviscid field is established, and it induces a spurious slip velocity (or equivalently a vortex sheet) at the boundary. The production of vorticity is materialized then at the following substep as the vortex sheet enters diffusively into the flow, eliminating the spurious velocity at the wall and enforcing the no-slip boundary condition. To illustrate this process consider the generation of vorticity over a wall segment due to the instantaneous blowing at one location (Fig. 2). According to Lighthill's model there is a slip velocity at the wall for an instant. A simple calculation shows that over an elementary wall segment δs we may calculate a circulation of $\delta\Gamma = U_{slip}\delta s$. The spurious slip velocity U_{slip} may be easily determined from inviscid flow theory, and at each location it is proportional to the inverse distance from the source. This spurious slip velocity is then nullified via the diffusive generation of vorticity at the wall so that the no-slip boundary condition is enforced. The amount of circulation that enters the flow over each time step δt, over each segment, is then $\delta\Gamma$ and it is related to a vorticity flux as $\delta\Gamma = \nu\partial\omega/\partial y\,\delta t\delta s$. Thus the instantaneous vorticity flux at each location over the wall due to the instantaneous blowing is expressed as:

$$\nu \left(\frac{\partial \boldsymbol{\omega}}{\partial \mathrm{y}}\right)_{\mathrm{w}} = -\frac{\mathrm{U_{slip}}}{\delta \mathrm{t}} \tag{7}$$

We consider now a system of sources/sinks at the wall of strength q_j that are distributed uniformly over a panel of size d_j, centered at locations $x'_j, j = 1, 2, 3, ...N$. The induced tangential velocity at point x_i on the wall and the corresponding vorticity flux may be determined as:

$$\nu\,\delta t\,\frac{\partial \boldsymbol{\omega}}{\partial \mathrm{y}}(\mathrm{x_i}) = \sum_{\mathrm{j=1}}^{\mathrm{N}} \frac{\mathrm{q_j}}{2\pi} \int_{-\mathrm{d_j}/2}^{\mathrm{d_j}/2} \frac{\mathrm{x}-\mathrm{s}}{(\mathrm{x}-\mathrm{s})^2}\,\mathrm{ds} \tag{8}$$

where $x = x_i - x'_j$. Similar expressions relate the vorticity flux at a location on the wall with the tangential acceleration of wall elements. It is also clear that via the present formulation the velocity gradients at the wall induced by the actuators may be determined as well and, ultimately, they can be used to affect the wall shear stresses.

For the purposes of our control scheme we consider a series of vorticity flux (or equivalently pressure gradient) sensors on the wall at locations $x_i, i = 1, 2, 3, ...M$. Using the formulas described above we can explicitly determine the actuator strengths necessary to achieve a desired vorticity flux profile at the wall, at a time instant k, by solving the linear set of equations:

$$B\, u_k \;+\; X_{k-1} \;=\; D_k \tag{9}$$

where $D_k = (\frac{\partial \omega^k}{\partial y}(x_1), \frac{\partial \omega^k}{\partial y}(x_2), ..., \frac{\partial \omega^k}{\partial y}(x_M))$ is an $M \times 1$ vector of the *desired* vorticity flux at the sensor locations, $X_{k-1} = (\frac{\partial \omega^{k-1}}{\partial y}(x_1), \frac{\partial \omega^{k-1}}{\partial y}(x_2), ..., \frac{\partial \omega^{k-1}}{\partial y}(x_M))$

is an $M \times 1$ vector of the *measured* vorticity flux at the sensor locations and $u_k = (q_1^k(x'_1), q_2^k(x'_2), ..., q_N^k(x'_N))$ is an $N \times 1$ vector of the source strengths at the actuator locations, B is an $M \times N$ matrix whose elements B_{ij} are determined by evaluating the integrals in Eq. 8 as:

$$B_{ij} \;=\; \frac{1}{2\pi}\,\mathrm{Log}\frac{|x'_j - x_i - d_j/2|}{|x'_j - x_i + d_j/2|} \tag{10}$$

Matrix B is a sparse matrix, and when large numbers of sensors and actuators are employed one may use multipole expansions to reduce the computational cost. Furthermore if the relative locations of the sensors and actuators remain constant, matrix B need be inverted only once, thus minimizing the computational cost of the method. Note that the location of sensors and actuators may be selected in such a way that the matrix B is *symmetric, positive definite*. By setting $D_k = (1+\alpha)X_k$, the solution of the above system of equations then implies the minimization of the functional

$$P(u_k) \;=\; \frac{1}{2}{u_k}^T B\, u_k \;-\; \alpha {u_k}^T X_k \tag{11}$$

The present technique gives us flexibility over the specific constraints that we wish to impose on the actuator strengths. Practical considerations may impose that control is performed only by jet-like actuators, $q_j \geq 0, j = 1, ..., N$ or that the blowing and suction configuration should result in a net zero mass flux;

$$\sum_{j=1}^{N} q_j \;=\; 0 \tag{12}$$

Such constraints may be easily incorporated in the above scheme by appropriately adjusting matrix B. A square matrix is always possible by modifying accordingly the number of sensors and actuators. In the present example the zero mass constraint was implemented so that $B_{Mj} = 1, \quad j = 1, ..., N$.

Sensors and actuators are not in the same locations. The simplicity of the present scheme allows for a number of different placement of sensors and actuators and the *active* selection of the optimal locations by suitable optimization algorithms. Here we chose the locations of sensors and actuators to be collocated. Physically this may be understood as a favorable situation as the sensors are able to sense the vorticity field induced by the actuators, allowing for the control scheme to suitably compensate for it.

2.3 Control of vortex dipole interactions with a wall

To illustrate the effects of the present control strategy on vortex-wall interactions, we consider the idealized situation of a two-dimensional vortex dipole interacting with a wall. This model has been used in the past by CMK and it allows us to compare our scheme with previous well established control strategies and draw some conclusions as to its efficiency.

We consider a Lamb's vortex dipole of radius R, traveling with velocity U. The Reynolds number of the initial vortex dipole is defined as $Re = UR/\nu$ and in all simulations discussed herein $Re = 400$, and the vortex is initially located at a distance of 2.5R above the wall. For the simulations presented herein we employ a fast high resolution viscous vortex method (Koumoutsakos and Leonard, 1995). No symmetry constraint is imposed on the evolution of the vorticity field, the time step is chosen as $\delta t = 0.01$, and the size of the Lagrangian vortex particles is chosen as $\epsilon^2 = 0.0002$. A maximum of 200,000 Lagrangian computational elements were used for these simulations. For more details on the implementation of fast viscous vortex methods and the selection of numerical parameters, the reader is referred to Koumoutsakos and Shiels (1996).

The sensors and actuators have a finite size. In our computational experiments we found that the sensed vorticity flux is more accurately described when we calculate its average over a finite segment of the wall and that the finite size of the actuators allows for a more well conditioned description of the velocity field near the wall. The effect of different actuator and sensor arrangements is assessed by considering here the following four configurations:

Configuration 1: Sensors of size 0.1 at $\pm(0.15 + 0.4i), i = 0, ..., 10$ for a total of 22 sensors and actuators at: $\pm(0.05 + 0.4i), i = 0, ..., 11$ for a total of 24 actuators.

Configuration 2: Sensors of size 0.1 at $\pm(0.15 + 0.2I), I = 0, ..., 19$ or a total of 40 sensors. Actuators, of size 0.1, at $\pm(0.05 + 0.2I), I = 0, ..., 20$ for a total of 42 actuators.

Note that in order to enforce the zero mass flux constraint one needs at least one more actuator than sensors. Because the present calculations are of a left-right symmetric flow, we enforce symmetry in the blowing/suction magnitude of the actuators. Hence the number of sensors and actuators in all configurations are related by $N/2 = M/2 + 1$.

Representative animations of the simulations discussed in the following section may be found at the www address:

`http://www.galcit.caltech.edu/~petros/RESEARCH/dipole.html`.

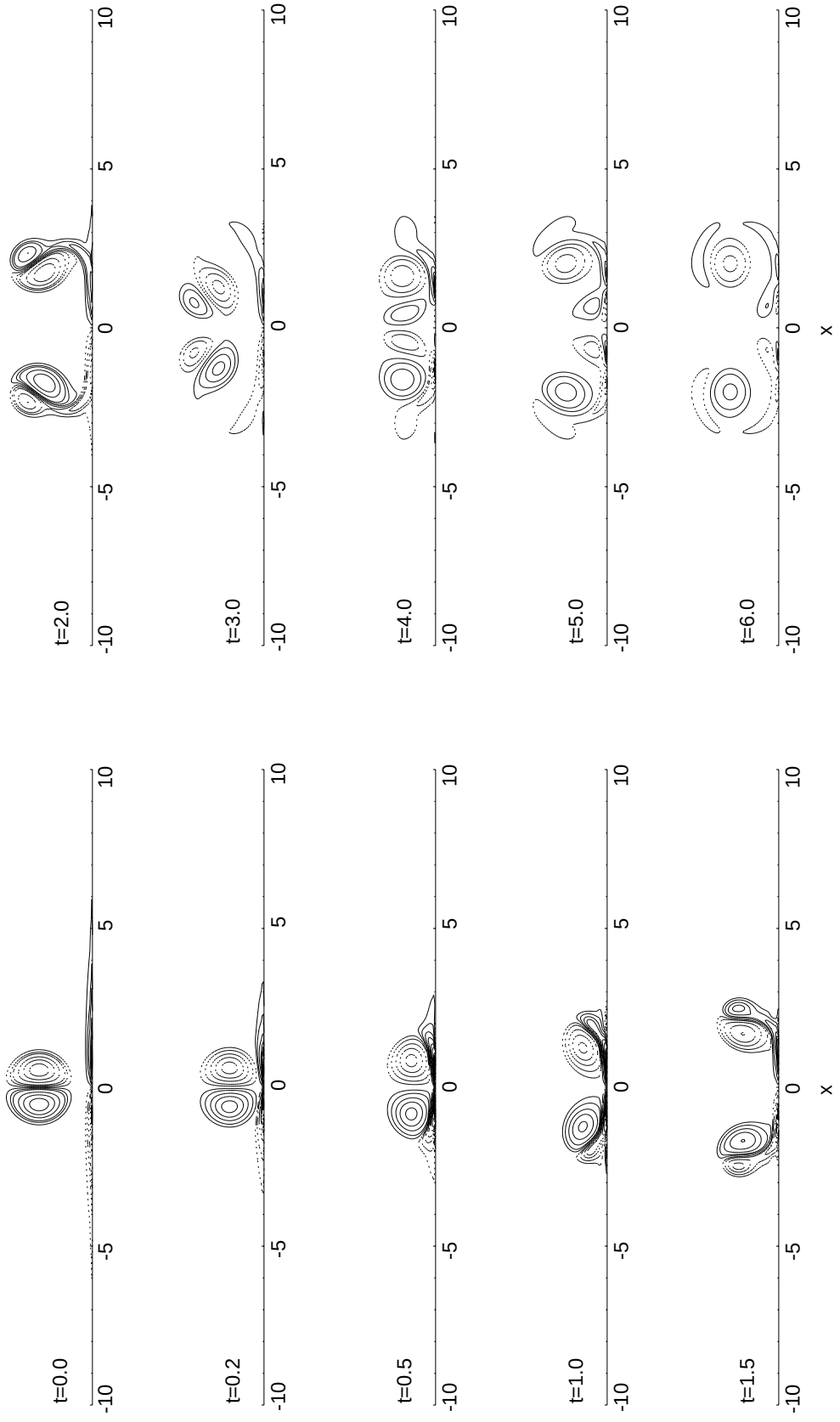

FIGURE 3. *Uncontrolled* interactions of a vortex dipole with a wall. Contours at t=0.2, 0.5, 1.0, 2.0, 3.0 ,4.0, 5.0, 6.0.

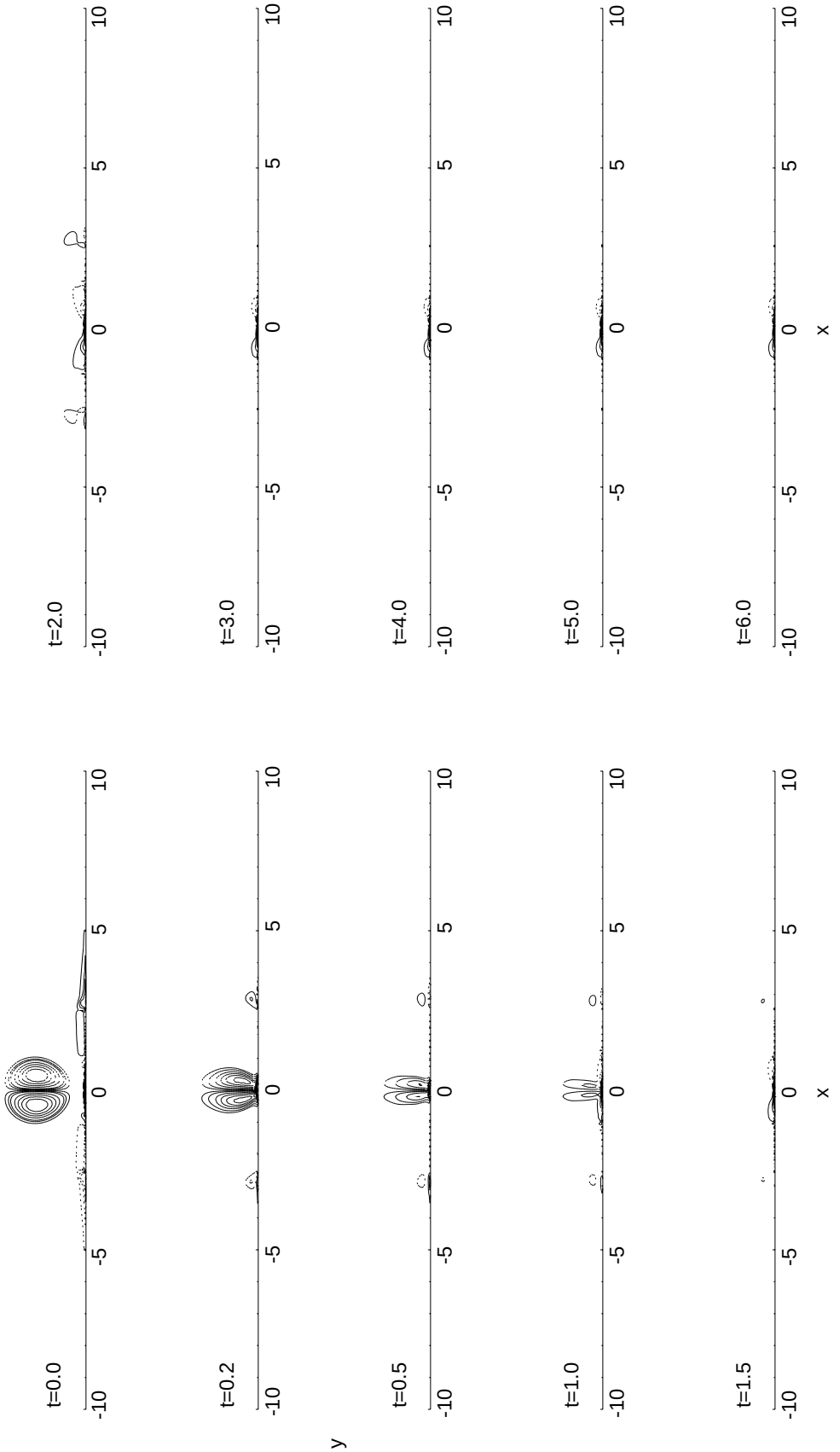

FIGURE 4. Configuration 1:*Controlled* wall-vortex interaction. Contours at t=0.2, 0.5, 1.0, 2.0, 3.0, 4.0, 5.0, 6.0.

2.4 Simulations of a vortex dipole interactions with a wall

No Control: In Fig. 3 we present contour plots of the vorticity field of the uncontrolled interaction of a vortex dipole with a wall. The vortex dipole propagates towards the wall generating vorticity of opposite sign on its surface. As the primary vortex approaches the wall, it interacts with this secondary vorticity generating two new dipoles that propagate outwards (T=0 to 1.5). When the initial components of the dipole are far apart, the new dipolar structures are lifted from the wall (T=1.5 to 2.0). The lifted secondary vorticity is weaker than the respective primary vorticity field. Thus, the preferential direction of the new dipoles results in an interaction between the original dipole components so that the vortical structures propagate again towards the wall (T=2 to 4). New secondary vorticity is generated and the process described before is repeated (T=4 to 5). However, due to the action of diffusion, the vorticity field is weakened (T= 5 to 6), resulting in a quasi-steady pattern that is eventually eroded.

The results of the present simulations are in excellent agreement with the results of Orlandi (1990) to which the reader is referred for a thorough discussion and quantification of this dipole wall interaction.

Control canceling the wall flux: In Fig. 4 we present contour plots of the vorticity field of the controlled interaction of a vortex dipole with a wall. In this type of control we eliminate the vorticity flux at the sensor locations (i.e. set $D_k = 0$). The vorticity flux is measured at each instant and at the following time step we appropriately adjust the strength of the actuators by solving

$$B\, u_k = -X_{k-1} \tag{13}$$

for u_k.

As the vortex descends towards the wall, the cancellation of the vorticity flux in the sensor locations results in a pattern where sinks are distributed in the middle of the wall. Respective blowing is established in the outer actuators so that the zero net mass flux is enforced (see also Fig. 5). As the control scheme acts to eliminate the secondary vorticity generated at the wall the primary vortex dipole 'sees' a permeable wall. At time T = 1.0 the primary vortex dipole has been drawn into the wall.

We examine here the effect of actuator placement in this type of control by using the sets of sensors and actuators locations described in Configuration 1 above. The locations of sensors and actuators are collocated and adjacent to each other. This allows for the sensors to account for the vorticity field generated by the actuators. As the present control strategy requires the elimination of the vorticity flux at the sensor locations, the actuator strengths are adjusted so that blowing/suction compensates to eliminate even the vortical structures generated by the actuators. The effect of sensor and actuator placement is discussed further in Koumoutsakos (1996).

The time invariance of the source/sink patterns at the wall suggests a weak time-correlation of the flow induced wall vorticity flux signals. The control scheme identifies the oncoming vortical structures and takes appropriate action to cancel the

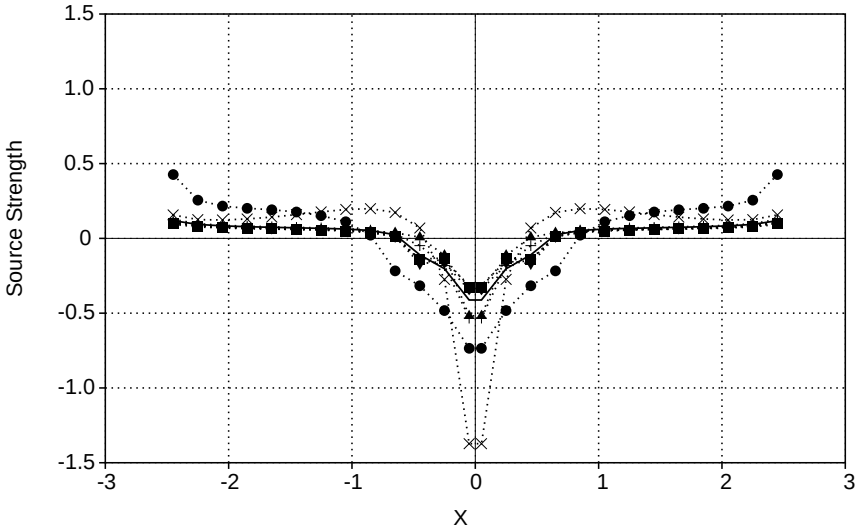

FIGURE 5. Configuration 1. Source strengths at times: • 0.2, × 0.5, ▲1.0, ▼2.0, ♦3.0, ■4.0, + 5.0,—— 6.0.

vorticity flux so that the dynamics of the flow are eventually governed by the dynamics of the actuators.

Control enhancing the wall flux: In Fig. 6 we present contour plots of the vorticity field of another type of controlled interaction of a vortex dipole with a wall. In this case the desired vorticity flux is such that the *secondary vorticity is enhanced* and the lift-off, observed in the uncontrolled case, is prevented. To achieve this, we require that the actuator strengths are adjusted so as to maintain the sensed vorticity flux (or equivalently $D_k = 2\,X_{k-1}$) via the solution of the system:

$$B\,\vec{u}_k = \vec{X}_{k-1} \tag{14}$$

Note that a simple sign change distinguishes Eq.13 and Eq.14.

The vorticity flux induced by the actuators at each time step is enforced to be equal to the vorticity flux induced by the flow at the previous time step. Hence the control scheme tries to maintain a steady profile of wall vorticity flux. The sensor and actuator locations are adjacent and collocated. They occupy segments of the wall up to ± 4.05, outside of which there are no sensors and actuators.

As the vortex dipole approaches the wall, it interacts with secondary vorticity. In this case, the primary vortex components roll on the sheet of secondary vorticity that the actuators try to maintain. Lift-off is prevented as the primary vortex components 'surf' the controlled portion of the wall. The vortical structures eventually lift off outside the controlled region, as the primary vortices have not lost enough of their strength by the act of diffusion. The lift-off process outside the controlled region is seemingly unaffected by the enhancement of the secondary vorticity. For example compare the last frame in Fig. 6 with the last frame in Fig. 3.

In Fig. 7 we present the actuator strengths for a series of time instances. Initially the actuator strengths are such that they oppose the descend of the vortex dipole.

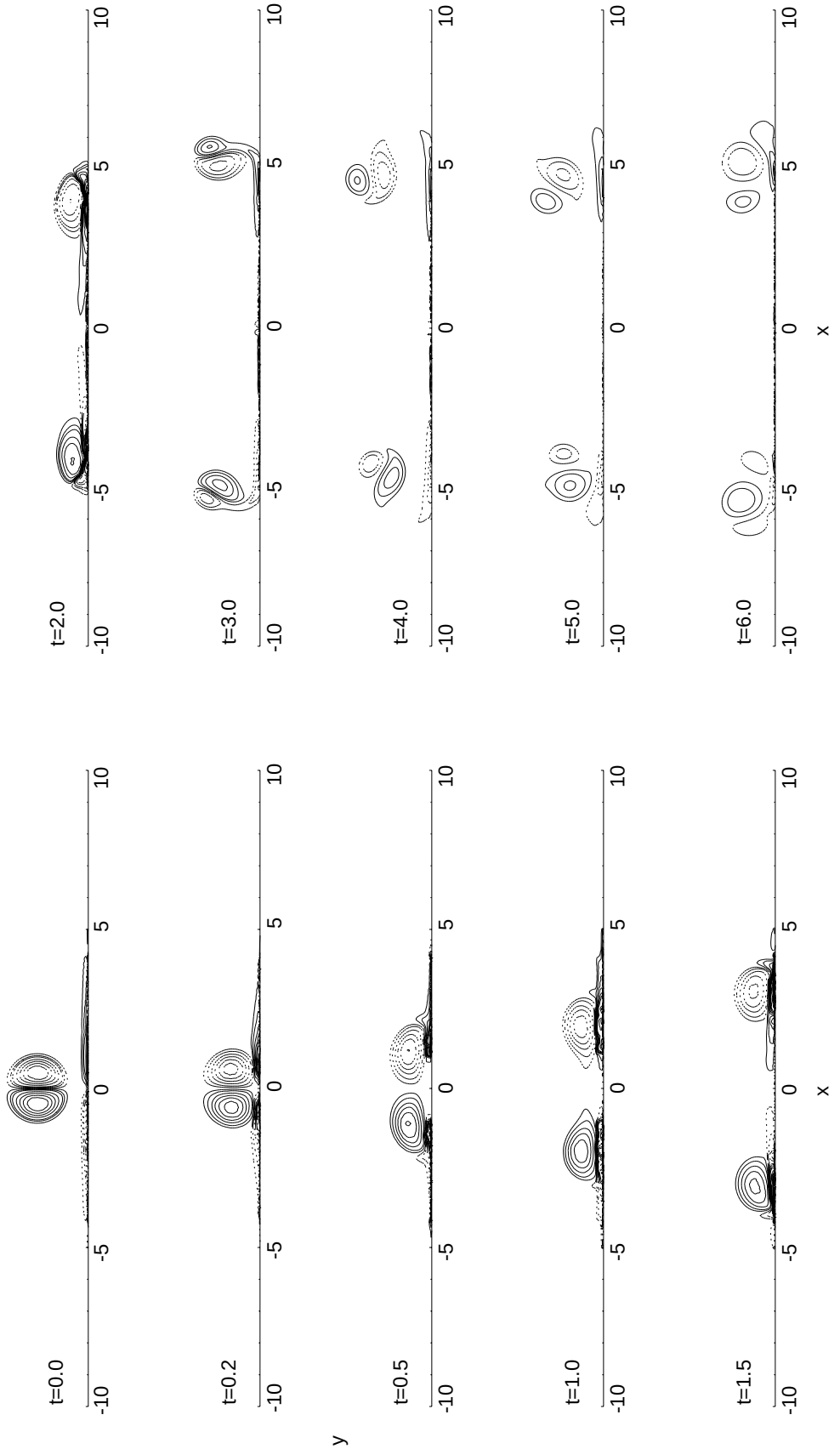

FIGURE 6. Configuration 2:*Controlled* wall-vortex interaction. Contours at t=0.2, 0.5, 1.0, 2.0, 3.0, 4.0, 5.0, 6.0.

As the secondary vorticity is enhanced and the primary vortices roll over the layer of secondary vorticity, the actuator strength is diminished.

Further studies of the effect of actuator and sensor placement is discussed in Koumoutsakos (1996).

We make here a comparison of the present active control strategy and the 'v-control', discussed by CMK. In their simulations of control of a vortex dipole impinging at a wall, the flow velocity normal to the wall is sensed at a distance $y^+ = 10$ off the wall. Bowing/suction is adjusted so as to oppose this velocity. As the primary vortex descends towards the wall, the blowing/suction counteracts this motion, enhancing the generation of secondary vorticity. This secondary vorticity in turn pairs off with the primary vortex, resulting in a vortex dipole propagating parallel to the wall. It appears that the center of the newly formed dipoles is near the $y^+ = 10$ location. This may explain also why the control scheme is not as effective, at say $y^+ = 25$, as then the sensed velocity field would not be that of the dipolar structure, but that of the primary vortex itself.

In CMK's simulations sensors and actuators are distributed throughout the wall and the lift-off of the secondary vorticity field is completely prevented. The behavior of the vorticity field is strikingly similar to the vorticity field presented here (Figs. 9, 10) over the controlled part of the wall. This strongly suggests that CMK's control strategy and the one discussed in the previous section are *equivalent*. Although they rely on two different descriptions of the same underlying physical mechanisms, they induce the same behavior to the vortical structures.

The two schemes differ in the way in which they sense the vorticity field that is approaching and adjust the necessary blowing/suction at the wall. As the present adaptive control strategy relies on the sensing of the wall pressure and the calculation of the vorticity flux, it appears more suitable to experimental applications and seems a more promising method for practical applications. The equivalence of the two schemes suggests that the successful results that have been obtained using the 'v-control' scheme in more complex flows (CMK, Lee *et al.* 1996) can be obtained more efficiently by the present strategy.

2.5 Formulation of adaptive control

The proposed adaptive control methodology relies on measurements of the wall vorticity flux at one time step and the immediate adjustment of the actuator strengths at the following time step to achieve a desired vorticity flux. This process may be improved either by considering earlier time signals of the vorticity flux in a systematic way or by identifying the time correlation of the vorticity flux signals at the sensor locations. Such correlations can then be conceptually represented by a nonlinear mapping as follows:

$$X_{k+1} = F(X_k, k) + Q(u_k, k) \tag{15}$$

where $F(\cdot)$ and $Q(\cdot)$ are the nonlinear maps of the vorticity flux and the control input respectively between the time instances $t = k\delta t$ and $t = (k+1)\delta t$.

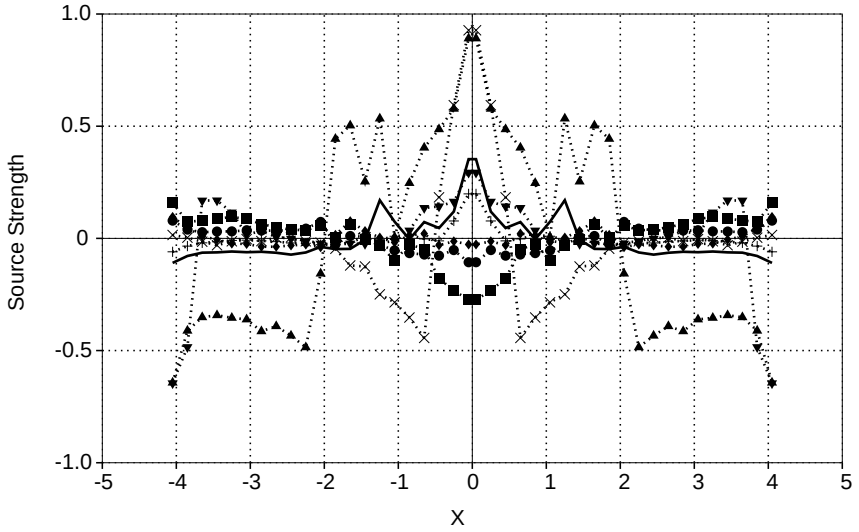

FIGURE 7. Configuration 2. For symbol captions see Fig. 5.

Taking advantage of the explicit relationship between the distributed mass sources and the vorticity flux (as was discussed in the previous sections) Eq. 15 may be expressed as:

$$X_{k+1} = F(X_k, k) + Bu_k \tag{16}$$

Then if $F(\cdot)$ is known, stabilization of the system becomes trivial by appropriately choosing the location of sensors and actuators as well as the number of constraints on the strength of the actuators to obtain a square and invertible matrix B. For example, one can use the feedback control $u_k = -B^{-1}F(X_k, k) + GX_k$ where G is a $n \times n$ matrix with all its eigenvalues inside the unit disk in the complex plane. The closed-loop system then is simply $X_{k+1} = GX_k$ which is asymptotically stable since all its eigenvalues have magnitude less than one.

The problem is then reduced to the *identification* of $F(\cdot)$. In Fig. 8 we present the function F for the uncontrolled case and for the controlled case 2b at a sensor location. It appears that after an initial transient, corresponding to the time that the primary vortex dipole is away from the wall, the dynamics of the system are determined by the dynamics of the actuators as F tends asymptotically to zero (or $F(X_k, k) \ll Bu_k$). On a related study Faller *et al.* (1994) have observed no strong time correlation of wall pressure signals in unsteady separated flows. This suggests that the identification of $F(\cdot)$ is not necessary and that one could proceed with the strategy discussed in the previous sections. We believe, however, that in order to account for experimental uncertainties and numerical errors and to increase the applicability of our scheme, the approximation/identification of the nonlinear map F is necessary.

There are two major approaches which can be used in order to achieve this. The *first* approach is based on approximating the nonlinear map at each instant by its first order, linear expansion according to $F(X_k, k) = A(k)X_k + \ldots$

The *second* approach is based on identification of $F(\cdot)$ using a non-linear neural

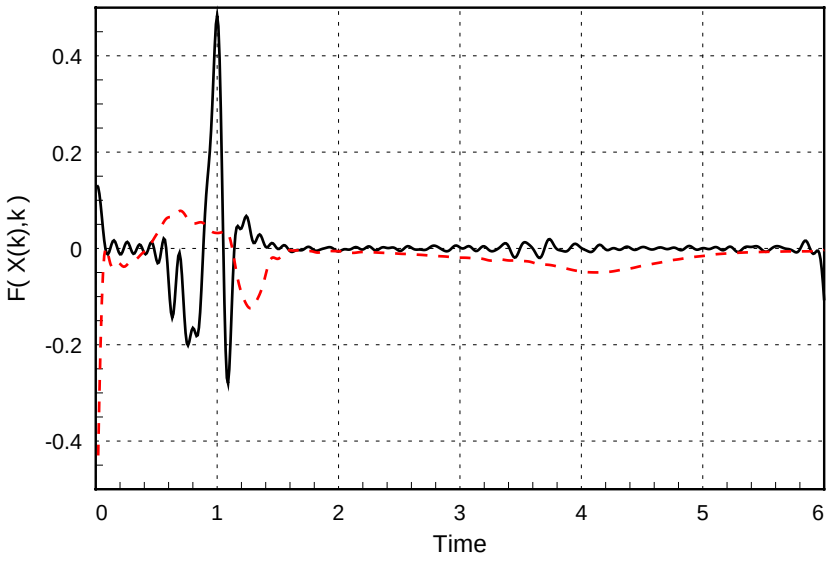

FIGURE 8. Residual function at location 1.15. ——— Controlled. Case 2, ---- No control.

network. Using past input and output data we can use neural network techniques to approximate the function $F(\cdot)$ adaptively. This approach is not as simple as the one in the linear approach, but it has the additional advantage of encompassing problems which require *shaping of the system response.*

Schreck *et al.* (1995) have demonstrated the ability of neural networks to capture and create simple models of the wall pressure field in unsteady separated flows of three dimensional airfoils. Moreover, they observed that the resulting model exhibits a strongly linear behavior.

3. Conclusions and future work

We have presented an active control technique that is based on the physical mechanism of vorticity generation at the wall. The wall vorticity flux may be used to describe the effects of several control devices such as (but not limited to) blowing and suction at the wall.

In the present scheme the vorticity flux is sensed at the wall via the measurement of wall pressure. A simple control strategy is described that allows calculation of the strength of wall transpiration in closed form to achieve a desired wall vorticity flux. The efficiency of the control scheme is demonstrated in simulations of the model problem of vortex dipole interactions with a wall. Using information available at the wall, the present control scheme is able to reproduce phenomena that were previously obtained computationally using off-wall information.

The implementation of the control scheme does not depend on a particular numerical method or flow configuration, making it suitable for practical applications. The simplicity of the technique and the explicit relationship between sensor and actuator outputs allows one to concentrate on issues such as devising strategies for optimal sensor and actuator placement. It may also be efficiently implemented

in control schemes employing large numbers of micro sensors and actuators as its computational cost is minimal. The present scheme may be easily applied to the control of a variety of wall bounded flows, and we believe that it could be effective in experimental control strategies.

Work is underway to implement the proposed strategy in the control of turbulent channel flow and in the control of unsteady separated bluff body flows.

REFERENCES

Andreopoulos, J. & Agui, J. H. 1996 Wall-vorticity flux dynamics in a two-dimensional turbulent boundary layer. *J. Fluid Mech.* **309,** 45-84.

Choi, H., Moin, P. & Kim, J. 1994 Active turbulence control for drag reduction in wall bounded flows. *J. Fluid Mech.* **262,** 75-110.

Faller, W., Schreck, S. & Luttges, M. 1994 Real time prediction and control of three-dimensional unsteady separated flow fields using neural networks. *AIAA Paper 94-0532.*

Gad-El-Hak, M. 1990 Control of low-speed airfoil aerodynamics. *AIAA J.* **118,** 1537-1552.

Ho, C. & Tai, Y. 1996 Review: MEMS and its applications for flow control. *J. Fluids Engr.* **118,** 437-447.

Hornung, H. 1990 *Sources of Vorticity.* Ae 232. Class notes, California Institute of Technology.

Johansson, A. V., Alfredsson, P. H. & Haritonidis, J. H. 1987 Evolution and dynamics of shear-layer structures in near-wall turbulence. *J. Fluid Mech.* **224,** 579.

Koumoutsakos, P., & Leonard, J. 1995 High resolution simulations of the flow around an impulsively started cylinder using vortex methods. *J. Fluid Mech.* **296,** 1-38.

Koumoutsakos, P., & Shiels, D. 1996 Simulations of the flow normal to an impulsively started and uniformly accelerated flat plate. *J. Fluid Mech.* **328,** 177-227.

Koumoutsakos, P. 1996 Active control of vortex-wall interactions. (Submitted to *Phys. Fluids A.)*

Lee, C., Kim, J., Babcock, D.& Goodman, R. 1996 Application of neural network to turbulence control for drag reduction. (Submitted for publication.)

Lighthill, M. J. 1963 *Introduction to boundary layer theory.* J. Rosenhead (editor) - Oxford University Press, New York. 54-61.

Löfdahl, L., Kälvesten, E. & Stemme, G. 1996 Small silicon pressure transducers for space-time correlation measurements in a flat plate boundary layer. *J. Fluids Engr.* **118,** 457-463.

Moin, P. & Bewley, T. R. 1994 Feedback control of turbulence. *Appl. Mech. Rev.* **47,** S3-S13.

MOIN, P. & KIM, J. 1985 The structure of vorticity fields in turbulent channel flow. Part 1. Analysis of instantaneous field and statistical correlations. *J. Fluid Mech.* **155,** 441-464.

ORLANDI, P. 1990 Vortex dipole rebound from a wall. *Phys. Fluids A.* **1429,** 75-110.

PANTON, R. L. 1984 *Incompressible Flow.* John Wiley and Sons, Inc.

SCHRECK, S., FALLER, W.,& LUTTGES, M. 1995 Neural network prediction prediction of three-dimensional unsteady separated flow fields. *J. Aircraft.* **32,** 178-185.

WU, J. Z., WU, X. H.,& WU, J. M. 1993 Streaming vorticity flux from oscillating walls with finite amplitude. *Phys. Fluids A.* **5,** 1933-1938.